Changes in Transcript Abundance in *Chlamydomonas reinhardtii* following Nitrogen Deprivation Predict Diversion of Metabolism[1][W][OA]

Rachel Miller[2], Guangxi Wu[2], Rahul R. Deshpande, Astrid Vieler, Katrin Gärtner, Xiaobo Li, Eric R. Moellering, Simone Zäuner, Adam J. Cornish, Bensheng Liu, Blair Bullard, Barbara B. Sears, Min-Hao Kuo, Eric L. Hegg, Yair Shachar-Hill, Shin-Han Shiu, and Christoph Benning*

Cell and Molecular Biology Program (R.M., G.W.), Department of Energy-Plant Research Laboratory (R.M., X.L., E.R.M.), Department of Plant Biology (R.R.D., X.L., B.B.S., Y.S.-H., S.-H.S.), and Department of Biochemistry and Molecular Biology (A.V., K.G., E.R.M., S.Z., A.J.C., B.L., B.B., M.-H.K., E.L.H., C.B.), Michigan State University, East Lansing, Michigan 48824

Like many microalgae, *Chlamydomonas reinhardtii* forms lipid droplets rich in triacylglycerols when nutrient deprived. To begin studying the mechanisms underlying this process, nitrogen (N) deprivation was used to induce triacylglycerol accumulation and changes in developmental programs such as gametogenesis. Comparative global analysis of transcripts under induced and noninduced conditions was applied as a first approach to studying molecular changes that promote or accompany triacylglycerol accumulation in cells encountering a new nutrient environment. Towards this goal, high-throughput sequencing technology was employed to generate large numbers of expressed sequence tags of eight biologically independent libraries, four for each condition, N replete and N deprived, allowing a statistically sound comparison of expression levels under the two tested conditions. As expected, N deprivation activated a subset of control genes involved in gametogenesis while down-regulating protein biosynthesis. Genes for components of photosynthesis were also down-regulated, with the exception of the *PSBS* gene. N deprivation led to a marked redirection of metabolism: the primary carbon source, acetate, was no longer converted to cell building blocks by the glyoxylate cycle and gluconeogenesis but funneled directly into fatty acid biosynthesis. Additional fatty acids may be produced by membrane remodeling, a process that is suggested by the changes observed in transcript abundance of putative lipase genes. Inferences on metabolism based on transcriptional analysis are indirect, but biochemical experiments supported some of these deductions. The data provided here represent a rich source for the exploration of the mechanism of oil accumulation in microalgae.

The search for sustainable sources of biofuels has led to renewed interest in microalgae as a potential feedstock and, consequently, a flurry of research has recently been initiated in microalgae (Wijffels and Barbosa, 2010). Microalgae accumulate large quantities of oils in the form of triacylglycerols (TAGs) when nutrient deprived, and a thorough analysis of the underlying molecular mechanism is currently in its infancy (Hu et al., 2008). At this time, *Chlamydomonas reinhardtii* is the premier microalgal molecular model for this analysis. As such, the formation of lipid droplets following nitrogen (N) deprivation has recently been documented in detail (Wang et al., 2009; Moellering and Benning, 2010). Although *C. reinhardtii* is not under direct consideration for the production of biomass as a biofuel feedstock, the analysis of its metabolism and physiology is expected to provide basic insights into mechanisms of TAG accumulation relevant to other microalgae at least of the green algal phylum.

The genome of *C. reinhardtii* is available (Merchant et al., 2007), and its annotation is currently at version 4 (http://genome.jgi-psf.org/chlamy/chlamy.home.html). At this time, a number of microarrays have been used to interrogate changes in response to environmental factors (Ledford et al., 2004, 2007; Jamers et al., 2006; Mus et al., 2007; Nguyen et al., 2008; Simon et al., 2008; Yamano et al., 2008; Mustroph et al., 2010). These microarrays could not cover all genes in the genome, but more recently, massively parallel cDNA sequencing approaches were applied to *C. reinhardtii*, overcoming the shortcomings of microarrays (González-Ballester et al., 2010). Likewise, we have chosen a cDNA sequencing-based approach using 454 and

[1] This work was supported by the U.S. Air Force Office of Scientific Research (grant no. FA9550–08–1–0165 to C.B.), by the U.S. National Science Foundation (grant nos. MCB–0749634 and MCB–0929100 to S.-H.S.), by a German Academic Exchange Program postdoctoral fellowship to S.Z., and by the Michigan State Agricultural Experiment Station.

[2] These authors contributed equally to the article.

* Corresponding author; e-mail benning@msu.edu.

The author responsible for distribution of materials integral to the findings presented in this article in accordance with the policy described in the Instructions for Authors (www.plantphysiol.org) is: Christoph Benning (benning@msu.edu).

[W] The online version of this article contains Web-only data.

[OA] Open Access articles can be viewed online without a subscription.

www.plantphysiol.org/cgi/doi/10.1104/pp.110.165159

Illumina technologies in parallel that allow the generation of large numbers of ESTs of varying abundance, which can be counted to obtain a measure of gene expression (Weber et al., 2007).

The goal of this study was to determine major changes in gene expression following N deprivation, the nutrient condition established in our previous analysis of lipid droplet formation and TAG accumulation in *C. reinhardtii* (Moellering and Benning, 2010). Comparison of the transcript levels of induced, N-deprived *C. reinhardtii* cultures with those of uninduced, N-replete cultures was expected to reflect the metabolic changes leading to TAG accumulation. Of course, making inferences about metabolism based on gene expression levels has its caveats, as gene expression does not necessarily directly translate into metabolic fluxes. To interrogate the meaningfulness of some of the transcript-level changes we observed with regard to metabolism, we also performed labeling experiments using acetate as the precursor. Acetate is a typical carbon source provided to *C. reinhardtii* for photoheterotrophic growth enabling short doubling times, and it is readily incorporated into fatty acids, the main constituents of TAGs. Keeping in mind that these are clearly conditions optimized for an experimental laboratory system, we nevertheless expect to be able to make basic inferences that will be relevant to a broader understanding of the induction of TAG biosynthesis and lipid droplet accumulation in green algae.

RESULTS

Defining Conditions for N Deprivation of *C. reinhardtii*

Ideally, one would like to use finely spaced time-course experiments to distinguish rapid versus long-term changes in gene expression following N deprivation. However, because our resources were limited, we decided to focus on two conditions, N replete and N deprived. Independent biological replicates allowed for statistically sound interpretations of the data. To determine the time point for N deprivation most likely to provide an accurate snapshot of readjustment of transcript steady-state levels following N deprivation, we first used northern-blot hybridization to compare the expression of genes known or expected to be regulated in *C. reinhardtii* following N deprivation. An ammonium transporter, AMT4, which has been previously shown to be activated by N deprivation (Mamedov et al., 2005), and two putative diacylglycerol acyltransferases, tentatively designated DGTT2 and DGTT3 (protein identifiers 184281 and 400751, genome version 4), were monitored to test the various conditions. RNA was isolated from cells grown in standard (10 mM NH_4^+) and low-N (0.5 mM NH_4^+) Tris-acetate phosphate (TAP) medium to impose N deprivation as well as from cells grown to mid-log phase in standard TAP medium, then transferred to either standard or no-N (0 mM NH_4^+) TAP, with samples taken at 24 and 48 h, to accomplish more drastic N deprivation (Fig. 1A). For standardization, equal amounts of RNA were loaded and the 18S rRNA abundance was examined. Although *C. reinhardtii* ribosomes turn over following N deprivation (Siersma and Chiang, 1971; Martin et al., 1976), their abundance drops no lower than 50% (see below). *AMT4* mRNA was absent from the uninduced cells and present at a high level in N-limited or N-deprived cells under the conditions tested. *DGTT2* mRNA was present at low levels in all conditions. *DGTT3* mRNA was present at low levels and increased slightly following N deprivation. N deprivation for 48 h showed the greatest difference in RNA levels compared with the N-replete cultures. Based on this basic analysis and our previous time-course study of lipid droplet formation and TAG accumulation (Moellering and Benning, 2010), a 48-h period of N deprivation was chosen to compare global transcript levels in N-replete and N-deprived cells.

Global Characteristics of *C. reinhardtii* Gene Expression following N Deprivation

To determine the differential expression of genes in *C. reinhardtii* under N-replete and N-deprived conditions, two sequencing approaches, 454 and Illumina, were applied. (The complete combined data set for both experiments is provided in Supplemental Spreadsheet S1.) Read length is longer for 454, but the number of reads per run is lower. As shown in Table I, 60- to 85-fold more sequence tags were generated with Illumina than with 454 sequencing. Among the 454 reads, 78% to 80% mapped to the *C. reinhardtii* genome. For the Illumina data, we mapped in three different ways, with varying stringency depending on whether 3′-end read quality and exon-spanning reads were considered. Without filtering reads, a substantially smaller proportion of Illumina reads (63%–68%) were mapped com-

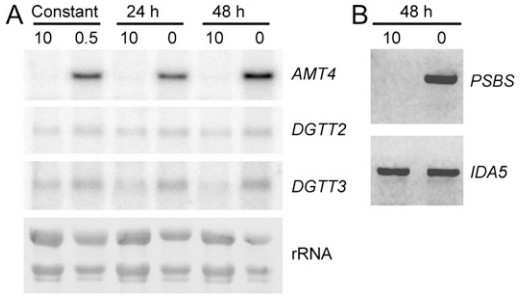

Figure 1. Transcript levels of specific genes. A, Cultures were grown in TAP medium that was N replete (10 mM NH_4^+; 10), continual N limited (0.5 mM NH_4^+; 0.5), or N deprived (0 mM NH_4^+; 0) for 24 or 48 h. The expression levels of *AMT4*, *DGTT2*, and *DGTT3* were measured by RNA-DNA hybridization, and rRNA was visualized as a loading control. B, Cultures were grown for 48 h in either N-replete or N-deprived conditions. The levels of *PSBS1* and *PSBS2* transcripts were measured using RT-PCR, and the constitutive *IDA5* gene served as a control.

Table I. *Summary of expression tags generated using two different sequencing methods*

Data Type	Sequencing Methods							
	454		Illumina					
Treatment[a]	N R	N D	T1	T2	T3	N1	N2	N3
Total[b]	$2.51 \times 10^{+05}$	$2.15 \times 10^{+05}$	$1.69 \times 10^{+07}$	$1.83 \times 10^{+07}$	$1.78 \times 10^{+07}$	$1.77 \times 10^{+07}$	$1.79 \times 10^{+07}$	$1.52 \times 10^{+07}$
Mapped[c]	$2.01 \times 10^{+05}$	$1.68 \times 10^{+05}$	$1.09 \times 10^{+07}$	$1.24 \times 10^{+07}$	$1.15 \times 10^{+07}$	$1.07 \times 10^{+07}$	$1.13 \times 10^{+07}$	$9.86 \times 10^{+06}$
Genic[d]	$1.08 \times 10^{+05}$	$1.32 \times 10^{+05}$	$8.96 \times 10^{+06}$	$9.43 \times 10^{+06}$	$1.02 \times 10^{+07}$	$8.33 \times 10^{+06}$	$8.82 \times 10^{+06}$	$7.81 \times 10^{+06}$
Intergenic[e]	$9.30 \times 10^{+04}$	$3.61 \times 10^{+04}$	$1.93 \times 10^{+06}$	$2.97 \times 10^{+06}$	$1.31 \times 10^{+06}$	$2.38 \times 10^{+06}$	$2.48 \times 10^{+06}$	$2.05 \times 10^{+06}$

[a]Treatment types: N R, T1, T2, and T3 represent N-replete growth; N D, N1, N2, and N3 represent N-deprived growth. For Illumina, there are three biologically independent replicates for each treatment (T1–T3 and N1–N3). [b]Number of sequencing reads after filtering out low-quality reads based on 454 and Illumina base-calling methods. [c]Number of sequencing reads after mapping to the *C. reinhardtii* version 4.0 genome. [d]Number of mapped sequencing reads overlapping with *C. reinhardtii* version 4.0-filtered gene models. [e]Number of mapped sequencing reads not overlapping with any *C. reinhardtii* version 4.0-filtered gene models

pared with 454 reads. Trimming low-quality 3′ regions of reads resulted in a further 2.7% decrease in the number of mapped reads. Despite the large number of unmapped Illumina reads, out of 16,710 *C. reinhardtii* gene models, 15,505 (92%) had one or more reads. In contrast, only 6,372 gene models (38.1%) were supported by the 454 transcriptome data set. In addition, nearly all genes covered by 454 were also covered by Illumina. Therefore, our sequencing data covered most annotated genes, enabling us to interrogate differential expression under normal conditions and following N deprivation. In addition, as expected, Illumina data provided a better coverage of the gene space than 454 sequences.

To determine differential gene expression following N deprivation, we modeled count data with a moderated negative binomial distribution (see "Materials and Methods"). Using thresholds of 5% or less false discovery rates and 2-fold or greater change for the Illumina data set, 2,128 and 1,875 genes were categorized as up- and down-regulated, respectively, following N deprivation. To see if fold changes inferred based on 454 and Illumina data sets were consistent, we determined the statistical correlation in fold change between these two data sets (Fig. 2) and found that it was rather weak (Pearson's correlation coefficient, $r^2 = 0.10$, $P < 2.2 \times 10^{-16}$). There was an apparent anomaly, as 4,313 genes (out of 6,369 genes with one or more reads from both data sets) had a high degree of up- and down-regulation, which was observed with the 454 but not the Illumina data set (Fig. 2A). Most of these genes with extreme

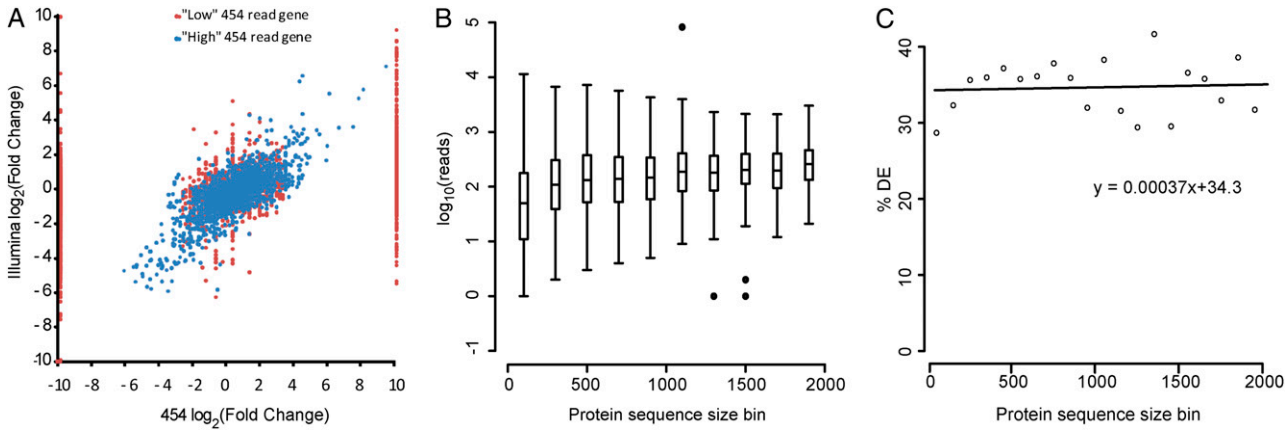

Figure 2. Fold change correlation between Illumina and 454 data sets and impacts of Illumina length bias on differential expression call. A, Only genes with one or more 454 and Illumina reads under either N-replete (+N) or N-deprived (−N) conditions were plotted. Fold change is determined by the number of reads following N deprivation divided by the number of reads under N-replete conditions for each gene. For genes with 2^{10}-fold or greater or 2^{-10}-fold or lesser changes, the fold change values were set to 10. Blue circles ("high" 454 read genes) indicate genes with 10 or greater 454 reads (+N and –N combined) and one or more 454 reads in both +N and –N. Red circles ("low" 454 read genes) indicate genes that did not satisfy one or both of the above criteria. B, Each box plot depicts the numbers of reads for protein-coding genes (log base 10) in a protein sequence size bin (0–2,000 amino acids, bin size of 100 amino acids). All proteins of 2,000 or more amino acids are classified as 2,000 amino acids. Outliers are shown in black circles. C, Percentage of genes that are regarded as differentially expressed (DE) in each protein sequence size bin. The line indicates the linear fit, and the equation for the line is shown as well.

responses based on 454 had very low counts (less than 10 reads combined in both conditions or zero reads in one of the conditions; Fig. 2A, red data points). As a result, high and likely inaccurate fold change values were assigned to those genes. In fact, if we only considered 2,056 genes with 10 or more reads combined and one or more reads in both conditions, the correlation between Illumina and 454 data was substantially improved ($r^2 = 0.57$, $P < 2.2 \times 10^{-16}$; Fig. 2, blue data points).

One important consideration in identifying differentially regulated genes is that there is a considerable transcript length bias in Illumina data. A longer transcript tends to have more reads than a shorter transcript expressed at the same level (Oshlack and Wakefield, 2009; Bullard et al., 2010). Consistent with earlier findings, we observed a significant correlation between the number of reads assigned to a protein sequence and its length (Spearman's rank $\rho = 0.33$, $P <$ 2.2e-16; Fig. 2B). Because of this length bias, longer transcripts may have more significant differences in differential gene expression studies and in some cases will lead to false-positive differential expression calls (Oshlack and Wakefield, 2009; Bullard et al., 2010). However, unlike previously published studies, we did not find a significant correlation between the percentage of genes differentially expressed and sequence length ($\rho = 0.09$, $P = 0.7$; Fig. 2C). This finding indicates that, although length bias remains an issue, our differential expression call may not be as significantly affected as reported previously.

Approximately 7% to 14% of the Illumina reads mapped to the "intergenic regions" (Table I). We assembled Illumina reads into 42,574 transcribed fragments (transfrags). Among them, 17,095 transfrags did not map with, or within the vicinity of (1,855 bases, 99th percentile intron length), current gene models. With the same conservative criterion, transfrags were joined into 1,828 "intergenic transcriptional units." Most importantly, 287 of these intergenic transcriptional units were up-regulated and 176 were down-regulated following N deprivation. These transfrags are unannotated genes that require further analysis to establish their authenticity.

Gene Ontology (GO) annotation was used to coarsely identify major categories of genes involved in particular biological processes to assess trends in their transcriptional regulation following N deprivation. We found multiple GO categories with significant enrichment in their numbers of differentially regulated genes (Table II). Particularly, genes associated with lipid metabolism tend to be up-regulated, while those involved in photosynthesis and DNA replication initiation tend to be down-regulated.

Table II. *GO categories significantly enriched in differentially regulated C. reinhardtii genes*

GO	Annotation	GO R[a]	No GO R[b]	GO U[c]	No GO U[d]	Reg[e]	P[f]	q[g]
GO:0006270 bp[h]	DNA replication initiation	9	926	0	6,633	Down	6.48×10^{-09}	4.51×10^{-06}
GO:0015995 bp	Chlorophyll biosynthetic process	8	927	0	6,633	Down	5.29×10^{-08}	2.76×10^{-05}
GO:0033014 bp	Tetrapyrrole biosynthetic process	6	929	0	6,633	Down	3.51×10^{-06}	7.32×10^{-04}
GO:0009765 bp	Photosynthesis, light harvesting	22	913	14	6,619	Down	5.72×10^{-12}	5.98×10^{-09}
GO:0015979 bp	Photosynthesis	23	912	0	6,633	Down	1.02×10^{-21}	2.13×10^{-18}
GO:0005576 cc[i]	Extracellular region	11	924	14	6,619	Down	8.28×10^{-05}	1.44×10^{-02}
GO:0009522 cc	PSI	4	931	0	6,633	Down	2.32×10^{-04}	3.23×10^{-02}
GO:0009538 cc	PSI reaction center	5	930	0	6,633	Down	2.85×10^{-05}	5.42×10^{-03}
GO:0009654 cc	Oxygen-evolving complex	6	929	0	6,633	Down	3.51×10^{-06}	7.32×10^{-04}
GO:0019898 cc	Extrinsic to membrane	4	931	0	6,633	Down	2.32×10^{-04}	3.23×10^{-02}
GO:0003755 mf[j]	Peptidyl-prolyl cis-trans-isomerase activity	21	914	32	6,601	Down	4.39×10^{-07}	1.83×10^{-04}
GO:0004600 mf	Cyclophilin	19	916	30	6,603	Down	2.29×10^{-06}	5.98×10^{-04}
GO:0016851 mf	Magnesium chelatase activity	4	931	0	6,633	Down	2.32×10^{-04}	3.23×10^{-02}
GO:0030051 mf	FK506-sensitive peptidyl-prolyl cis-trans-isomerase	19	916	30	6,603	Down	2.29×10^{-06}	5.98×10^{-04}
GO:0042027 mf	Cyclophilin-type peptidyl-prolyl cis-trans-isomerase activity	19	916	30	6,603	Down	2.29×10^{-06}	5.98×10^{-04}
GO:0006006 bp	Glc metabolic process	5	944	1	6,618	Up	1.65×10^{-04}	3.83×10^{-02}
GO:0006468 bp	Protein amino acid phosphorylation	117	832	501	6,118	Up	2.37×10^{-06}	2.47×10^{-03}
GO:0006629 bp	Lipid metabolic process	18	931	38	6,581	Up	9.92×10^{-05}	2.59×10^{-02}
GO:0004672 mf	Protein kinase activity	113	836	479	6,140	Up	2.08×10^{-06}	2.47×10^{-03}
GO:0004713 mf	Protein-Tyr kinase activity	85	864	342	6,277	Up	8.04×10^{-06}	4.20×10^{-03}
GO:0004674 mf	Protein Ser/Thr kinase activity	92	857	391	6,228	Up	2.50×10^{-05}	7.46×10^{-03}

[a]GO R, Number of significantly up- or down-regulated (R) genes with the GO annotation in question. [b]No GO R, Number of significantly up- or down-regulated genes without the GO annotation. [c]GO U, Number of genes without significant expression change with the GO annotation. [d]No GO U, Number of genes with no significant expression change that do not have the GO annotation. [e]Reg, Direction of regulation (N deprived compared with N replete). [f]Fisher's exact test P value. [g]The q value is calculated using the R package q value. [h]bp, Biological process. [i]cc, Cellular component. [j]mf, Molecular function.

Induction of Gametogenesis and Sexual Reproduction

Because N deprivation triggers gametogenesis (Martin and Goodenough, 1975; Kurvari et al., 1998), we examined several genes known to be involved in mating-type plus (mt^+) gamete differentiation or sexual fusion in *C. reinhardtii* as internal controls for the induction state of the cells following N deprivation (Supplemental Table S1). Following N deprivation, cells had substantial increases in the abundance of transcripts of four of the six genes considered. These genes encode FUS1, which is a glycoprotein required for sex recognition, SAG1 (the mt^+ agglutinin gene), peptidase M gametolysin, which releases the gametes from the cell wall, and NSG13, which is a protein of unidentified function known to be expressed in gametes, as summarized by Harris (2009b). A second gametolysin gene (encoding peptidase M11) and *GSP1*, which encodes a gamete-specific transcription factor, did not show increased expression following N deprivation, but perhaps that is because only a single time point was examined.

Effects on Genes of N Metabolism and Protein Biosynthesis

Many genes involved in N import and assimilation are known to be induced following N deprivation (Schnell and Lefebvre, 1993; González-Ballester et al., 2004; Fernandez et al., 2009). Our analysis revealed greater than 2-fold up-regulation for several genes, including those that encode NO_3^- and NO_2^- transporters and reductases, as well as transport systems for NH_4^+ and organic N sources (Supplemental Table S2). Of the genes involved in assimilation of NH_4^+ by the Gln synthetase-Glu synthase cycle, only *GLN3* was up-regulated. Similarly, most genes involved in amino acid biosynthesis did not show a greater than 2-fold change. Thus, transcript abundance suggests that following N deprivation, pathways for the acquisition of new N sources are strongly up-regulated, whereas biosynthetic pathways that utilize the assimilated N remain relatively unaffected.

Decades ago, N deprivation of *C. reinhardtii* was found to result in degradation and resynthesis of both cytoplasmic and chloroplast ribosomes (Siersma and Chiang, 1971; Martin et al., 1976). Both the rRNA and proteins of the ribosomes were turned over under the conditions of N deprivation that also induce gamete differentiation. Hence, we expected that the mRNAs for the ribosomal proteins might show different steady-state levels in the comparison of logarithmically growing cells and cells that have been N deprived for 48 h. Indeed, following N deprivation, the abundance of transcripts encoding proteins of the chloroplast ribosomes consistently decreased to 30% to 50% of their levels of expression in logarithmically growing cells (Supplemental Table S3).

A subset of the cytosolic 80S ribosomal protein genes has been identified in the version 4.0 genome data set. Among those that have been annotated, most are encoded by single-copy genes (Supplemental Table S4), although a few have two copies (e.g. *L7*, *L10*, *L13*, and *L23*). As these gene products are assembled into ribosomes, the respective genes have high levels of constitutive expression. The abundance of the transcripts in vegetative cells and N-deprived cells was fairly similar, although they are listed in the table starting with those that have the most elevated expression in the latter.

The RPL22 ribosomal protein of the cytosolic ribosomes is encoded by a multigene family in *C. reinhardtii*. Of the 37 *RPL22* genes in version 4.0 of the genome data set, 13 appeared not to be expressed under either condition tested and six had barely detectable levels of transcripts. Of the 18 remaining genes, two gave rise to the most predominant transcripts (Supplemental Table S5, yellow highlighting), and their transcripts did not change markedly in abundance. Four of the 18 genes were moderately expressed, and their transcript levels doubled in the N-deprived cells (Supplemental Table S5, light blue highlighting). Six of the 18 genes had markedly lower levels of transcripts following N deprivation (Supplemental Table S5, light green highlighting), while six others showed relatively constant levels of expression (Supplemental Table S5, medium blue highlighting). The *RPL22* genes are scattered among at least six chromosomes, and no correlation was found between location and level of gene expression.

General Changes in Primary Metabolism

Changes in transcript abundance of genes encoding enzymes of primary metabolism are depicted in Figure 3 and summarized in Supplemental Table S6. Transcripts encoding key enzymes of the glyoxylate cycle, gluconeogenesis, and the photosynthetic carbon fixation cycle markedly decrease following N deprivation. Transcript abundance for the glyoxylate cycle enzymes isocitrate lyase and malate synthase decreased more than 16-fold. In addition, mRNA abundance of the cytosolic (predicted) phospho*enol*pyruvate carboxykinase, which catalyzes the committed reaction of gluconeogenesis, dropped to 25% of the levels in N-replete cells, as did transcripts encoding enzymes involved in carbon fixation and reduction, ribulose-bisphosphate carboxylase, sedoheptulose 1,7-bisphosphate aldolase, and sedoheptulose-bisphosphatase. In contrast, there was a considerable increase in the transcript abundance of the cytosolic enzyme pyruvate phosphate dikinase. This is a key enzyme in the C4 photosynthetic pathway and is regulated by light. It has also been associated with suppressed phospho*enol*pyruvate carboxykinase activity (Osterås et al., 1997) and salt stress (Fisslthaler et al., 1995). Recently, this enzyme has been shown to play an important role in N remobilization (Taylor et al., 2010). Likewise, the transcript abundances for enzymes of the pentose phosphate cycle predicted to be localized in the cyto-

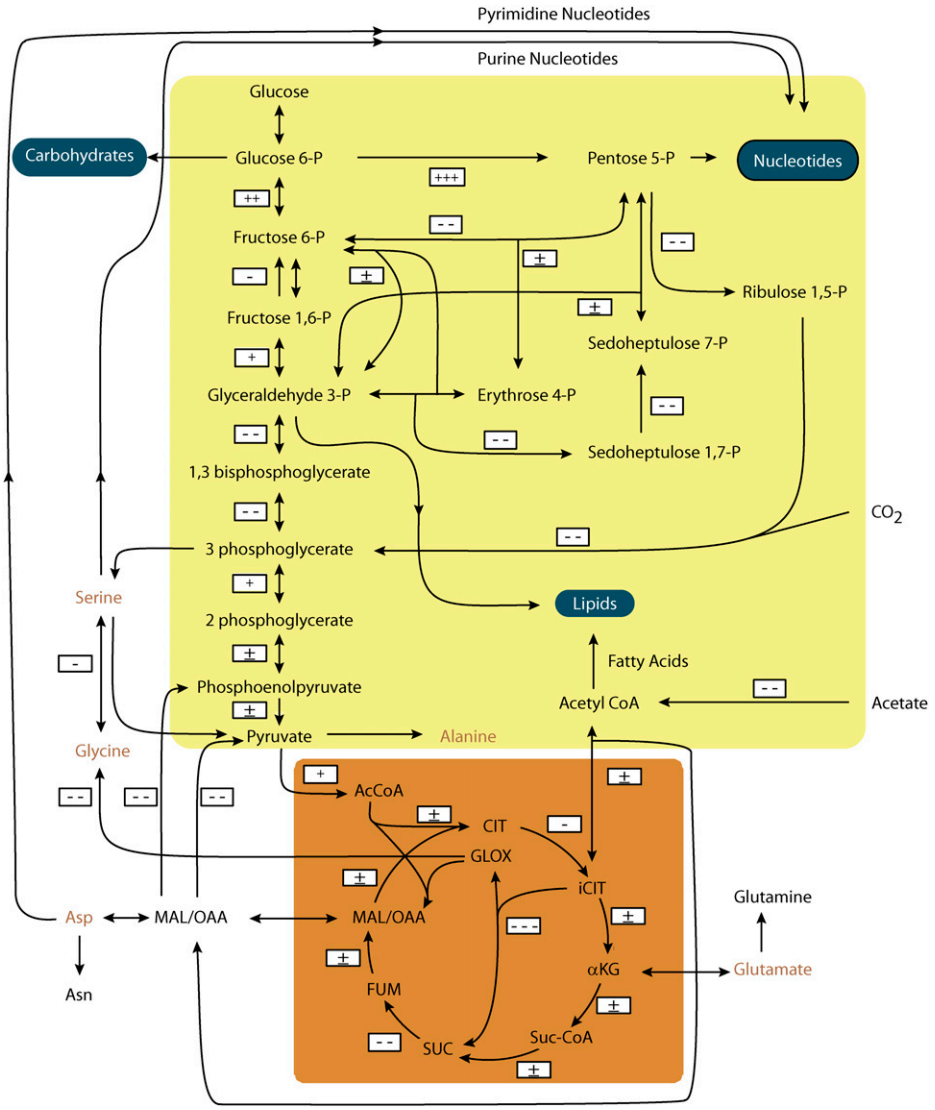

Figure 3. Regulation of genes involved in primary metabolism. The figure indicates the central metabolic pathways of *C. reinhardtii* and gives the differential regulation of gene expression following N deprivation. Symbols represent $\log_2$ fold change as follows: +++, greater than 5; ++, greater than 2 and less than 5; +, greater than 1; ±, less than 1 and greater than −1; −, less than −1; −−, less than −2 and greater than −5; −−−, less than −5.

sol, Glc-6-P 1-dehydrogenase and phosphogluconate dehydrogenase (decarboxylating), were increased under those conditions. The mRNA encoding for one of the pyruvate decarboxylase subunits represented in the data set was also increased in abundance following N deprivation. The pyruvate decarboxylase complex converts pyruvate to acetyl-CoA, which is a precursor of fatty acid biosynthesis. Genes for other enzymes of the glycolytic pathway, such as pyruvate kinase, did not show very drastic changes in response to the N deprivation.

To verify whether the changes observed in RNA abundance actually reflect changes in the activity of glyoxylate and gluconeogenic pathways, cells were grown in the presence of [U-^{13}C]acetate. As the cells take up acetate as a carbon source, the distribution of the ^{13}C in the cellular metabolites gives an insight into the activity of the pathways leading to them. The intracellular amino acids as well as the sugar units of the carbohydrates and RNAs were analyzed with gas chromatography-mass spectrometry (GC-MS) as described in "Materials and Methods" (Fig. 4). The natural abundance refers to the naturally occurring distribution of ^{13}C in the molecule. The mass isotopomers M0, M1, M2, etc. refer to molecules having, respectively, zero, one, two, etc. atoms of ^{13}C.

Cells grown in N-replete medium showed a higher degree of labeling in Ser and Gly than did N-deprived cells (Fig. 4). The fully labeled fraction (M3) accounted for almost 80% of the total Ser in the cells grown in N-replete medium. Hence, most of the Ser was derived from the gluconeogenic pathway, which incorporates the labeling of acetate into the glycolytic intermediate 3-phosphoglycerate, a precursor of Ser. There was also about 10% of M2 Ser. This probably derived from the reaction catalyzed by the reversible Ser hydroxylmethyltransferase, which favors the production of Ser from Gly (Mattingly et al., 1976). The Gly in this reaction would mostly be fully labeled (M2; Fig. 4), largely from the glyoxylate cycle, hence giving rise to

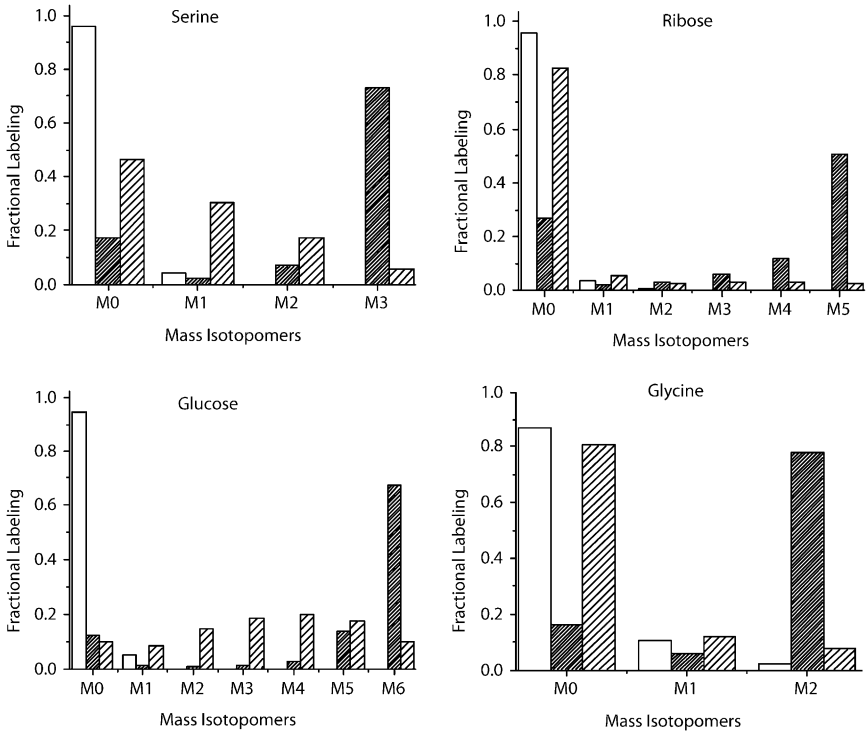

Figure 4. Changes in labeling patterns reflecting changes in gene expression. Labeling of metabolites after 24 h of N deprivation compared with N-replete cells is shown. The metabolites give an indication of the pathway activity. Intracellular Ser and Gly were extracted by quick quenching and extraction with cold methanol. Rib and Glc were obtained from the acid hydrolysis of RNA and cellular polysaccharides, respectively. The labeling was analyzed by GC-MS after derivatization. Natural labeling refers to the naturally occurring distribution of ^{13}C in the molecule. The mass isotopomers M0, M1, M2, etc. refer to molecules having, respectively, zero, one, two, etc. atoms of ^{13}C. White bars, Natural labeling; fine cross-hatched bars, N-replete cells; coarse cross-hatched bars, N-deprived cells.

M2 Ser. In cells grown in N-deprived medium, we observed a markedly lower incorporation of the ^{13}C atoms into the amino acids. Almost 80% of Gly was unlabeled (M0), indicating a very low activity of the glyoxylate cycle. Similarly, N-deprived cells had reduced label in carbohydrates and Rib. Since these molecules were formed essentially by the gluconeogenic pathway during growth in the medium employed, the N-deprived cells appeared to have much lower gluconeogenic activity. Thus, these biochemical data corroborated the transcript abundance data (Fig. 3) that suggested a down-regulation of the glyoxylate and gluconeogenic pathways in N-deprived cells.

No appreciable change in transcripts for genes encoding components of the mitochondrial respiratory pathway was noted following N deprivation. However, an 11-fold increase in the transcript abundance of an alternative oxidase gene (*AOX1*) was observed, while the *AOX2* transcript was down-regulated 4-fold. These findings were consistent with previous observations of changes in gene expression of *AOX1* and *AOX2* (Baurain et al., 2003).

The candidate genes for peroxisomal β-oxidation showed an overall decrease in their transcript levels following N deprivation, with acyl-CoA oxidase and 3-oxoacyl-CoA thiolase (*ATO1*) transcript abundance decreasing most drastically (greater than 3-fold). The only exception was an enoyl-CoA oxidase/isomerase candidate gene (*ECH1*), which showed increased transcript levels (greater than 2-fold; Supplemental Table S8). An apparent down-regulation of fatty acid oxidation is in line with the accumulation of TAGs under these conditions.

Reduced Transcript Abundance for Most Photosynthetic Genes

In *C. reinhardtii*, photosynthetic efficiency decreases following N deprivation, at least partially due to a reduction in the abundance of light-harvesting complexes (Plumley and Schmidt, 1989; Peltier and Schmidt, 1991) and selective degradation of the cytochrome b_6f complex (Bulté and Wollman, 1992; Majeran et al., 2000). Likewise, the abundance of transcripts encoding photosynthesis-related proteins was substantially reduced following N deprivation. This regulation was not restricted to light-harvesting complexes and cytochromes but extended to the two photosystems as well (Supplemental Table S7). Following N deprivation, the steady-state level of all nucleus-encoded PSI genes decreased by at least 6-fold, while the abundance of transcripts from genes encoding the corresponding light-harvesting proteins was decreased even further, resulting in a 19- to 43-fold decrease relative to N-replete conditions. Only four of the cytochrome subunits are encoded by the nuclear genome, and three of them showed a considerable down-regulation (6-fold) following N deprivation. In contrast, the transcript levels of *PETO* were weakly increased (2-fold). This observation supports the hypothesis that this protein may have a regulatory role as opposed to being a functional cytochrome b_6f subunit (Hamel et al., 2000), because the PETO protein is only loosely bound to the complex and its function is not required for the oxidoreductase activity. Expression of all nuclear genes encoding PSII components also decreased following N deprivation (Supplemental Table S7), although the two

least abundant transcripts decreased only slightly. The PSII light-harvesting complex encoding transcripts showed a comparable change in abundance. Most of the transcript levels were reduced, while the weakly expressed *LHCB7* gene showed no alteration in transcript levels.

The only two genes of the light-harvesting complex of PSII not following that pattern were *PSBS1* and *PSBS2*. Their transcript levels were strongly increased following N deprivation (119- and 52-fold, respectively). This result was confirmed by reverse transcription (RT)-PCR (Fig. 1B).

Specific Changes in Gene Expression Related to General Lipid Metabolism

N deprivation has been demonstrated to lead to the accumulation of TAG in specialized organelles as well as to structural changes and breakdown of the intracellular membrane systems such as the thylakoids and the endoplasmic reticulum (ER; Martin et al., 1976; Moellering and Benning, 2010). Therefore, we expected this to be reflected in the expression of genes encoding enzymes of lipid metabolic pathways. However, changes in transcript levels of genes encoding fatty acid metabolism (Supplemental Table S8) were modest (Fig. 5). A 2-fold increase in transcript levels for ketoacyl-acyl carrier protein (ACP) synthetase was observed. This enzyme is part of the fatty acid synthase II complex that catalyzes the acyl-ACP-dependent elongation steps from C4 to C14 in higher plants. The gene for acyl-ACP thioesterase (FAT1) also showed elevated transcript levels following N deprivation (about 4-fold). Its reaction terminates fatty acid synthesis by cleaving the acyl chain from ACP. This reaction competes with the direct transacylation of ACP by glycerol-3-phosphate acyltransferases for the formation of phosphatidate. An increase in FAT1 activity, therefore, could be indicative of increased fatty acid export from the chloroplast to the ER, where TAG assembly occurs, as acyl-ACPs have to be hydrolyzed prior to export (Pollard and Ohlrogge, 1999).

A strong increase in transcript levels was observed for the gene encoding the committing step of TAG synthesis. Out of the five putative diacylglycerol acyltransferases genes identified in the version 4.0 genome data set, only four were expressed under either or both growth conditions (Supplemental Table S8). One of these genes (*DGTT1*, PID 285889) was almost completely suppressed under N-replete conditions but showed a large increase in transcript abundance following N deprivation. However, its overall transcript abundance was too low to be detected by northern blot compared with other genes encoding putative diacylglycerol acyltransferases, which were much less differentially expressed, consistent with the initial RNA-DNA hybridization analysis (Fig. 1A).

Phosphatidic acid phosphatase takes part in the Kennedy pathway of glycerolipid and TAG synthesis (Fig. 5). Both of the two candidate genes for phosphatidic acid phosphatase in *C. reinhardtii* annotated in the version 4.0 data set showed increased transcript levels following N deprivation. Both are part of the PAP2 family, which is thought to have a broad substrate specificity (Carman and Han, 2006). The increase in the expression of the presumed phosphatidic acid phosphatase genes is consistent with the notion that DAG is generated from phosphatidic acid for further TAG biosynthesis following N deprivation.

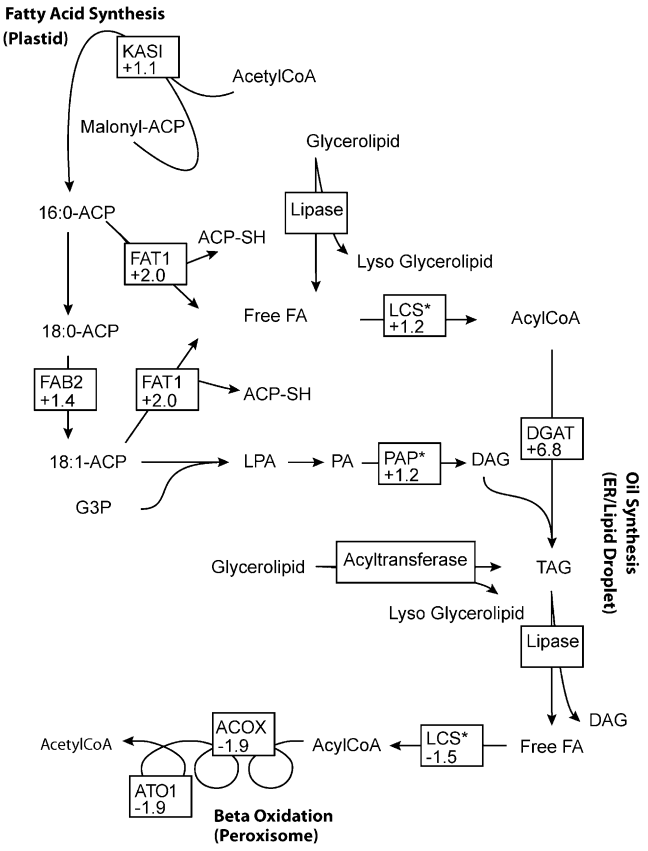

Figure 5. Selected changes in glycerolipid metabolism transcript abundance. Numbers indicate $\log_2$ fold change of transcript abundance following N deprivation. Enzymes labeled with an asterisk cannot be unequivocally assigned to a specific step in the metabolic pathway and are hypothetical.

Out of a total of 16 putative membrane-bound desaturase- and hydroxylase-encoding genes found in *C. reinhardtii*, only three showed a change in transcript abundance that is greater than 2-fold. Transcript abundance for microsomal Δ12-desaturase was more than 3-fold higher following N deprivation, as was that for the plastidic acyl-ACP-Δ9-desaturase, which introduces the first double bond in an acyl chain. Other microsomal desaturase-encoding transcripts, such as that encoding FAD13, an $\omega 13/\Delta 5$-desaturase, were also slightly increased in abundance, whereas the plastid desaturase-encoding genes were not affected.

Of all lipid-related genes, those encoding putative lipases showed the strongest differences in transcript

abundance between the two conditions tested. By searching for "lipase," "phospholipase," or "patatin" through the version 4.0 genome sequence data, 130 proteins containing the GXSXG motif common to hydrolases were identified. Among the respective genes, 35 (27%) showed increased and 11 (8.5%) showed decreased transcript levels by 2-fold or more following N deprivation. Supplemental Table S8 lists these 46 most strongly differentially regulated lipase candidates. In addition, many potential lipases may be considered constitutively expressed. Seventy-four out of 130 (57%) lipase candidates were expressed at slightly higher levels following N deprivation. Some of these genes may encode lipases that are important for the turnover or replacement of membranes during cell growth or gamete fusion.

Changes in RNA Abundance for Transcription Factors

The Plant Transcription Factor Database (Pérez-Rodríguez et al., 2010) was used to identify 386 genes encoding putative transcription factors and transcriptional regulators in the *C. reinhardtii* transcript data set, which could be sorted into 53 families (Table III). Of the 368 genes, 83 showed a 2-fold or greater change in transcript abundance following N deprivation, with 46 being up-regulated and 37 being down-regulated.

To date, only a few of the putative transcription factors identified in the *C. reinhardtii* genome have a known function. Transcript abundance for the gene encoding NIT2, a transcription factor regulating nitrate metabolism, was increased 6-fold, while that for NAB1, a transcription factor regulating light-harvesting proteins, was decreased 16-fold, consistent with previously described physiological changes in response to N deprivation (Mussgnug et al., 2005; Camargo et al., 2007). The transcript level for the GSP1 mt^+ gamete-specific transcription factor was decreased 3-fold at the 48-h sample point. When looking at the changes in RNA abundance of putative transcription factor genes, no obvious trends emerged. However, transcripts falling into the AP2-EREBP and bHLH families were generally more abundant following N deprivation, while those of the FHA family were generally decreased.

DISCUSSION

Microalgae such as *C. reinhardtii* undergo drastic changes in metabolism and ultimately development when N deprived. Some of the most remarkable changes involve gametogenesis (Harris, 2009b) and metabolic changes that lead to the accumulation of TAGs (Hu et al., 2008). The former aspect has been studied since the 1970s. However, focus on the latter has been largely motivated by the renewed interest in microalgae as biofuel feedstocks (Wijffels and Barbosa, 2010). As sequencing technology has become increasingly fast and affordable, comparison of transcriptomic changes under different experimental conditions by massive parallel sequencing of cDNA libraries is a viable first approach toward identifying genes that define changes in response to N deprivation or other nutrient stresses (González-Ballester et al., 2010). With the goal of gaining a better understanding of the factors underlying or even controlling the process of TAG accumulation following N deprivation, the focus has to be on metabolism and genes that encode enzymes of relevant pathways or regulatory factors.

The validity of making inferences on metabolism from transcriptome data in this study has been verified in different ways. First, specific genes known to be induced following N deprivation, such as genes involved in gametogenesis or ammonium transport, were found to be expressed as described previously. Second, major metabolic changes predicted by transcript analysis, such as the redirection of acetate from the glyoxylate cycle and gluconeogenesis to fatty acid biosyntheses following N deprivation (Fig. 3), were corroborated by labeling experiments (Fig. 4).

By and large, gross changes in transcript abundance in response to N deprivation follow expected themes: genes encoding enzymes directly involved in N metabolism or N compound uptake have to be induced, protein biosynthesis is reduced to adjust to the decreased availability of amino acids, and photosynthesis is down-regulated to adjust to the altered metabolic state of the cell. In cyanobacteria, N deprivation led to the degradation of the highly abundant phycobili light-harvesting proteins so that they could be used as an N source for protein synthesis (Collier and Grossman, 1992). In *C. reinhardtii*, there is evidence that the cytochrome subunits are degraded not in response to the low concentrations of N per se but rather to the changed energy content of the cell. Thus, one possible advantage for the cells to decrease photosynthesis following N deprivation is to prevent the accumulation of reactive oxygen species (Bulté and Wollman, 1992). At the same time, genes encoding proteins of the respiratory chain in mitochondria were only moderately affected following N deprivation except for those encoding alternative oxidases, which showed elevated transcript abundance. These enzymes are induced under a number of stress conditions that affect the redox environment of the cell, but these effects can be quite indirect and are often difficult to causally connect to the applied stress, in this case N deprivation. It should also be pointed out here that only the expression of nuclear genes is probed in this study; the expression levels of genes for organelle-encoded proteins relevant to respiration or photosynthesis have not been examined.

A Role for PSBS following N Deprivation?

One particular surprise was the strong up-regulation of *PSBS* following N deprivation in *C. reinhardtii*. In Arabidopsis (*Arabidopsis thaliana*), PSBS has been shown to play a critical role in nonphotochemical

Table III. *Illumina analysis of transcripts encoding transcription factors and regulators following N deprivation*

PID[a]	Annotation[b]	TID[a]	T +N[c]	T −N[c]	Log_2FC[d]	FDR[e]
Transcription factors						
115124	SBP	115124	3	0	−26.5	4.2×10^{-01}
425069	CPP	399885	332	5	−5.9	5.1×10^{-23}
126810	NAB1, involved in the light-regulated differential expression of the light-harvesting antenna, CSD	126810	23,357	1,253	−4.1	3.5×10^{-36}
119948	MYB-related	119948	50	3	−4.0	1.5×10^{-07}
191829	FHA	191829	221	15	−3.8	1.2×10^{-14}
147364	CCAAT	147364	119	9	−3.6	4.7×10^{-10}
290169	bZIP	290176	10,444	895	−3.4	6.9×10^{-28}
154254	FHA	154254	302	26	−3.4	9.0×10^{-12}
119194	MYB-related	119194	11	1	−3.4	3.1×10^{-02}
285394	FHA	285401	2,150	207	−3.3	4.3×10^{-23}
426624	bZIP	397080	10,907	1,271	−3.0	2.1×10^{-21}
119283	MYB-related	119283	96	12	−2.9	1.9×10^{-08}
194555	C3H	194555	1,764	336	−2.3	2.9×10^{-09}
415440	VARL	411514	843	162	−2.3	6.2×10^{-11}
417527	C2C2-GATA	413714	103	23	−2.1	1.1×10^{-05}
96716	SBP	96716	12	3	−1.9	8.4×10^{-02}
426728	MYB-related	399133	22	6	−1.8	3.3×10^{-02}
186803	GSP1; gamete-specific transcription factor, HB	186803	980	289	−1.7	1.3×10^{-04}
423729	FHA	397389	391	114	−1.7	1.4×10^{-05}
112237	MYB	112237	502	155	−1.6	3.5×10^{-06}
407701	S1Fa-like	425995	363	120	−1.5	2.0×10^{-04}
104804	CPP	104804	29	10	−1.4	3.8×10^{-02}
285882	bZIP	285889	1,004	367	−1.3	2.0×10^{-04}
149734	C2H2	149734	6,593	2,748	−1.2	1.2×10^{-03}
171165	TIG	171165	16,705	7,723	−1.0	1.8×10^{-03}
415443	bHLH	409330	181	332	1.0	7.9×10^{-03}
393055	bZIP	421105	21	39	1.0	1.0×10^{-01}
393622	bHLH	420168	317	593	1.0	6.7×10^{-03}
399062	HSF	422722	1,776	3,323	1.0	1.8×10^{-03}
186995	RWP-RK	186995	3,085	5,907	1.0	7.9×10^{-04}
416794	AP2-EREBP	410803	313	612	1.1	2.4×10^{-03}
426843	PLATZ	397100	80	158	1.1	6.8×10^{-03}
298349	MYB-related	298356	451	912	1.1	2.8×10^{-03}
205561	MYB-related	205566	5,271	11,132	1.1	1.4×10^{-02}
147286	bZIP	147286	906	1,889	1.2	2.8×10^{-04}
419111	C3H	412152	329	704	1.2	3.5×10^{-04}
342954	MYB-related	342961	757	1,636	1.2	2.2×10^{-04}
130971	G2-like	130971	300	680	1.3	3.5×10^{-04}
417388	MYB-related	413124	1,291	2,917	1.3	1.5×10^{-04}
187531	bZIP	187531	803	1,897	1.3	2.2×10^{-04}
189471	CCAAT	189471	79	189	1.4	3.8×10^{-04}
196473	G2-like	196473	551	1,349	1.4	1.1×10^{-05}
415966	MYB-related	409909	4	10	1.4	2.7×10^{-01}
321493	TAZ	321500	9,879	25,105	1.4	5.9×10^{-04}
205919	AP2-EREBP	205924	23	61	1.5	4.1×10^{-03}
347478	None	347485	931	2,593	1.6	1.8×10^{-05}
205871	C2C2-GATA	205876	1,867	5,390	1.6	3.7×10^{-07}
19751	AP2-EREBP	19751	297	925	1.7	1.1×10^{-06}
183777	bHLH	183777	6,895	21,726	1.8	1.3×10^{-08}
290479	SBP	290486	189	616	1.8	1.8×10^{-07}
195916	RWP-RK	195916	11	36	1.8	6.8×10^{-03}
284832	MYB-related	284839	142	532	2.0	6.3×10^{-09}
148404	AP2-EREBP	148404	1,324	5,634	2.2	1.4×10^{-10}
414856	SBP	411130	1,520	6,689	2.2	2.8×10^{-12}
146990	VARL	146990	14	61	2.2	3.8×10^{-05}

(*Table continues on following page.*)

Table III. (*Continued from previous page.*)

PID[a]	Annotation[b]	TID[a]	T +N[c]	T −N[c]	Log_2FC[d]	FDR[e]
205642	NIT2, nitrate-regulated transcription factor	205647	1,366	7,924	2.6	7.5×10^{-18}
117291	MYB	117291	117	740	2.8	1.1×10^{-13}
195838	RWP-RK	195838	108	718	2.8	3.4×10^{-16}
116658	MYB-related	116658	56	452	3.1	2.9×10^{-16}
153934	bHLH	153934	82	705	3.2	2.5×10^{-19}
195891	RWP-RK	195891	404	3,825	3.3	8.9×10^{-25}
424240	C3H	397539	19	273	3.9	8.7×10^{-19}
118761	SBP	118761	1	42	5.5	2.4×10^{-08}
405949	bHLH	390447	10	1,821	7.6	4.3×10^{-62}
177225	bHLH	177225	7	1,666	8.0	1.2×10^{-62}
Transcriptional regulators						
206670	SNF2	206677	106	7	−3.8	3.3×10^{-09}
143060	PHD	143060	332	24	−3.7	2.1×10^{-15}
401818	PHD	417802	7	2	−1.7	3.5×10^{-01}
325701	TRAF	325708	3,740	1,118	−1.6	3.2×10^{-07}
146398	TRAF	146398	372	113	−1.6	5.6×10^{-06}
169174	SNF2	169174	209	67	−1.5	8.1×10^{-05}
287740	PHD	287747	3	1	−1.5	7.9×10^{-01}
377090	GNAT	377097	821	290	−1.4	3.9×10^{-04}
151030	TRAF	151030	406	156	−1.3	4.1×10^{-04}
142283	HMG	142283	11,647	4,587	−1.2	1.7×10^{-03}
142152	GNAT	142152	189	80	−1.1	4.7×10^{-03}
172711	SET	172711	549	233	−1.1	3.5×10^{-03}
115484	SET	115484	39	71	1.0	5.8×10^{-02}
193146	TRAF	193146	1,032	1,899	1.0	2.5×10^{-03}
145759	TRAF	145759	503	1,004	1.1	2.2×10^{-03}
154505	SET	154505	1,304	2,760	1.2	4.5×10^{-04}
308637	PHD	308644	20	49	1.4	1.3×10^{-02}
188181	TRAF	188181	265	723	1.5	3.5×10^{-06}
282628	GNAT	282635	584	1,684	1.6	2.1×10^{-06}
192899	HMG	192899	1,261	4,097	1.8	3.7×10^{-08}
205788	GNAT	205793	215	782	2.0	1.4×10^{-09}
423513	HMG	398414	149	1,178	3.1	2.5×10^{-19}
321619	PHD	321626	0	2	26.0	$1.0 \times 10^{+00}$
143723	GNAT	143723	0	3	26.6	2.5×10^{-01}

[a]PID and TID are the protein and transcript identifiers for each gene model for *C. reinhardtii* genome version 4.0. [b]Annotation indicates gene name, family, or predicted function. [c]T +N and T –N are the total number of hits for each gene model, from either N-replete or N-deprived conditions. [d]Log_2FC is the log to base 2 of the difference in hits between the two conditions, for each gene model. [e]FDR refers to the false discovery rate for each gene model.

quenching (Li et al., 2000, 2002), but previous studies in *C. reinhardtii* have not detected either of the two PSBS proteins in the thylakoids, and nonphotochemical quenching was shown to be independent of these proteins (Bonente et al., 2008). Only rarely have ESTs been found for *PSBS* transcripts, with the exception of the cDNA stress collection II, which contains RNAs from different stress treatments, including the switch from ammonium to nitrate (Shrager et al., 2003; Bonente et al., 2008). Our results indicate that *PSBS* expression in *C. reinhardtii* is induced by ammonium deprivation, as was observed previously for the expression of the gene for alternative oxidase, *AOX1* (Baurain et al., 2003).

Recycling of Membrane Lipids or de Novo Synthesis of TAGs?

The elevation of synthesis and export of fatty acids from the chloroplast following N deprivation could indicate that TAG is assembled from fatty acids that are synthesized de novo. This step would require the activation of the fatty acids by a long-chain acyl-CoA synthetase. In fact, increased abundance of RNA encoding a putative long-chain acyl-CoA synthetase was observed, and the respective protein has been identified in the lipid droplet proteome (Moellering and Benning, 2010). However, another enzyme that could contribute to the changing spectrum of fatty acids is a putative phospholipid/glycerol acyltransferase, for which the transcript level decreased during N deprivation. Long-chain acyl-CoA synthetases are likely to play a key role in determining the fate of fatty acids in the cell (Shockey et al., 2002). Regulation of the respective genes could be a major factor in controlling the flux of fatty acids toward glycerolipid synthesis and their degradation by β-oxidation.

Major intracellular changes occur following N deprivation, and these are likely accompanied by remodeling of membranes. Thus, fatty acids in membrane lipids might be recycled into TAGs. Consistently, some of the transcripts whose abundance changes the most were those encoding putative lipases. In general, lipases belong to a family of enzymes that deesterify carboxyl esters, such as TAGs and phospholipids. As TAGs accumulate following N deprivation, TAG lipases would be expected to be down-regulated. However, classifying lipases with selective substrate specificity based solely on their primary sequences is challenging, a fact that needs to be taken into consideration when interpreting our data set. A TAG lipase typically contains a Ser-Asp/Glu-His catalytic triad, with the Ser catalytic center located in a GXSXG motif (Brady et al., 1990; Winkler et al., 1990). Some recently characterized TAG lipases in animals, yeast, and plants contain a patatin-like, iPLA2 family Ser-Asp catalytic dyad (Zimmermann et al., 2004; Athenstaedt and Daum, 2005; Eastmond, 2006; Kurat et al., 2006). Genes encoding lipases specific for membrane lipids would be expected to be up-regulated, as they might mobilize fatty acids from membrane lipids into TAGs. Moreover, signaling pathways involving lipid products generated by lipases, such as diacyglycerol, may also control steady-state TAG levels (Kanoh et al., 1993). Further biochemical characterization of some of the most regulated lipase candidate genes will be necessary to determine their role in TAG accumulation following N deprivation.

On the other hand, we recognize that lipase expression or activities may also be controlled at the posttranscriptional level, including translational regulation and posttranslational modifications of the encoded proteins. In mammals, a hormone-sensitive lipase is phosphorylated by protein kinase A upon cAMP elevation and consequently exhibits better accessibility to lipid droplets (Holm et al., 2000). Some of the *C. reinhardtii* TAG lipases may have a similar regulatory pattern and hence not show significant transcriptional changes when cells are N deprived. Reverse genetic studies on the lipase candidates and forward genetic screens for mutants with TAG deficiency phenotypes will disclose the bona fide TAG lipases and other lipases that impact TAG metabolism.

It should also be noted that during the analysis of the lipid gene data set, the annotation ambiguities of several fatty acid desaturases became obvious in the version 4.0 genomic sequence data set: the *C. reinhardtii* genome harbors four presumed paralogs of FAD5 (named FAD5a–FAD5d). Based on our current prediction analysis (Emanuelsson et al., 1999) and previous reports (Riekhof et al., 2005; Riekhof and Benning, 2009), FAD5a and FAD5b are presumed to be targeted to the chloroplast, whereas FAD5c and FAD5d are likely located in the ER membrane. However, experimental corroboration is still needed.

CONCLUSION

Our interpretation of this data set places emphasis on TAG metabolism and potential regulatory factors, which are undoubtedly not yet completely identified. We expect that others will be able to mine this data set, taking into account different biological processes pertaining to N deprivation. Cross-querying this data set with a lipid droplet proteomics data set (Moellering and Benning, 2010) should further narrow the possible candidates relevant for TAG accumulation. Likewise, a meta-analysis of this and other data sets, including those from other species, could facilitate the identification of genes most likely involved in TAG accumulation, as was recently done for low-oxygen stress (Mustroph et al., 2010). Thus, this study represents only a first step of many toward gaining a molecular understanding of TAG accumulation and other cellular changes triggered by N deprivation in *C. reinhardtii*.

MATERIALS AND METHODS

Strains and Growth Conditions

The *Chlamydomonas reinhardtii* strain used was dw15.1 (cw15, nit1, mt^+), kindly provided by Arthur Grossman. The cells were grown in liquid cultures under continuous light (approximately 80 μmol photons m^{-2} s^{-1}). For N-replete growth, TAP medium (Harris, 2009a) with 10 mM NH_4^+ (TAP + N) was used. For preliminary experiments, N deprivation was applied by two methods: continuous growth in TAP with 0.5 mM NH_4^+ or growth in TAP + N to 5×10^6 cells mL^{-1}, followed by transfer to TAP with no NH_4^+ (TAP − N) for an additional 24 or 48 h. For further experiments, N deprivation was defined as growth in TAP + N to 5×10^6 cells mL^{-1}, followed by transfer to TAP − N for 48 h.

For labeling studies, the cells were grown in 500-mL shaker flasks with a culture volume of 50 mL with continuous shaking. For the N deprivation experiment, cells were first grown in TAP medium with unlabeled acetate with at least five cell doublings to mid logarithmic phase to reach a biomass equivalent to 0.3 to 0.4 g cell dry weight L^{-1}. The cells were divided up and transferred to TAP medium containing [U-^{13}C]acetate (Isotec), either TAP + N or TAP − N.

Sequencing Read Processing

To generate material for high-throughput sequencing, cells were grown in 100 mL of TAP + N to 5×10^6 cells mL^{-1}. The cultures were split in half, and cells were collected by centrifugation, with one pellet being resuspended in 50 mL of TAP + N and the other in 50 mL of TAP − N. After 48 h, the total RNA was harvested using a Qiagen RNeasy Plant Mini kit. The RNA samples were treated with Qiagen RNase-free DNase I during extraction.

For 454 sequencing, full-length cDNA pools were generated with the Clontech SMART cDNA library construction kit. cDNA was synthesized using a modified cDNA synthesis primer (5′-TAGAGACCGAGGCGGCCGACATGTTTTGTTTTTTTTTCTTTTTTTTTTVN-3′). Full-length cDNAs were amplified by PCR and pooled to increase their concentration. An *Sfi*I digest was performed, followed by size fractionation. Fractions with the highest intensity and size distribution were pooled and purified. The resulting cDNA pools were then submitted to the Michigan State University-Research Technologies Service Facility for sequencing on a 454 GSFLX Titanium Sequencer (454 Life Sciences). For Illumina sequencing, total RNA was submitted directly to the Michigan State University-Research Technologies Service Facility for sequencing on an Illumina Genome Analyzer II (Illumina).

Default parameters were used to pass reads using 454 and Illumina quality-control tools. The filtered sequence data were deposited in the National Center for Biotechnology Information Short Read Archive with the reference series number GSE24367 and subseries numbers GSE24365

and GSE24366 for the Illumina and the 454 data sets, respectively. The filtered 454 sequencing reads were mapped to the *C. reinhardtii* version 4.0 assembly from the Joint Genome Institute with GMAP (Wu and Watanabe, 2005). In GMAP, the maximum intron length was set at 980 bp, which is at the 95th percentile of annotated *C. reinhardtii* intron lengths. The Illumina reads were mapped with Bowtie (Langmead et al., 2009) using parameters as follows: two or fewer mismatches, sum of Phred quality values at all mismatched positions at 70 or less, and excluding reads mapped to one or more locations. Because the sequence qualities of Illumina reads degrade quickly toward the 3′ end, an alternative mapping data set was generated with reads trimmed from the 3′ end (until the 3′-end-most position with Phred-equivalent score was 20 or greater). Trimmed reads of less than 30 bp were excluded from further analysis. In addition to sequence quality issues, some reads may span two exons and would not be mapped by Bowtie correctly. We used TopHat (Trapnell et al., 2009) to identify these exon-spanning reads to generate another set of read mapping. The information from TopHat was used for assembling mapped reads into transfrags with Cufflinks (Trapnell et al., 2010). In Cufflinks, the maximum intron length was set at 1,855 bp (99th percentile of all the intron lengths), 5% minimum isoform fraction, and 5% pre-mRNA fraction. Transfrags within 1,855 bp of an existing *C. reinhardtii* version 4.0 gene model were regarded as potential missing exons of annotated genes. The rest were regarded as intergenic exons, and adjacent transfrags less than 1,855 bp apart were joined into "transcriptional units."

Northern-Blot Analysis and RT-PCR

Total RNA was harvested from N-replete or N-deprived cells as described above, and 4 μg of each total RNA was separated on a 1% formaldehyde gel and transferred to a Hybond-N^+ nylon membrane (GE Healthcare). Probes were synthesized from cDNA and labeled with ^{32}P using the Amersham Megaprime labeling kit (GE Healthcare). The blots were hybridized with the labeled probes in Ambion ULTRAhybe (Applied Biosystems/Ambion) at 42°C overnight. The blots were washed twice for 5 min with low-stringency buffer (1× SSC and 0.1% SDS) at 60°C and then twice for 5 min with high-stringency buffer (0.1× SSC and 0.1% SDS) at 60°C. The blots were exposed to a Molecular Dynamics phosphor screen (GE Healthcare) overnight and visualized with a Storm 820 phosphor imager (GE Healthcare). Probes were synthesized from cDNA for AMT4 (5′-GTATTGCGTCCGATCTGC-3′ and 5′-CGTGGAAATGCTGTAGGG-3′), DGTT2 (5′-TAAAGCACCGA-CAAATGTGC-3′ and 5′-CATGATCTGGCATTCTGTGG-3′), and DGTT3 (5′-GGTGGTGCTCTCCTACTGGA-3′ and 5′-CCATGTACATCTCGGCA-ATG-3′).

For RT-PCR, RNA was extracted from N-replete and N-deprived cultures using TRIzol reagent (Invitrogen) and subjected to DNase treatment with the Turbo DNA-free kit from Ambion. A total of 1 μg of DNA-free RNA was used for cDNA synthesis with the Invitrogen Moloney murine leukemia virus reverse transcriptase. A total of 0.5 μg of oligo$(dT)_{12–18}$ primer (Invitrogen) and 0.5 μg of random hexamer primers (Promega) were added to the RNA, and the volume was adjusted to 20 μL final volume. After heating the samples at 70°C for 10 min, they were incubated on ice for 5 min. Twenty units of RNase inhibitor (Applied Biosystems), 20 nmol of deoxyribonucleotide triphosphates (Invitrogen), 4 μL of first-strand buffer, and 0.2 μmol of dithiothreitol were added to the reaction. The reaction mixture was incubated at 37°C for 10 min for primer annealing. A total of 200 units of Moloney murine leukemia virus reverse transcriptase was added, and the reaction was incubated at 37°C for 1 h followed by deactivation at 70°C for 10 min. A total of 1 μL of a 1:10 dilution of the respective cDNA was used as template for a PCR using GoTaq polymerase (Promega). The reaction mixture (25 μL) contained 1× buffer, 5 nmol of deoxyribonucleotide triphosphates, 12.5 pmol of each primer, and 1 unit of polymerase. PCR cycle conditions were 3 min of initial denaturation at 94°C, following 40 cycles of 30 s of denaturation, 30 s of annealing at 60°C, and 3 min of elongation at 72°C. Final elongation was performed at 72°C for 10 min. The *PSBS*-specific primers (5′-ATGGCCATGACTCTGTCGAC-3′ and 5′-TTAGGCGGACTCCTCGTCC-3′) amplify both *PSBS1* and *PSBS2*. The *IDA5* gene (5′-GCCAGGTCTCTGCTCTGGTG-3′ and 5′-TACTCGGACTTGGC-GATCCA-3′) served as a control.

Analysis of Differential Gene Expression

Differential expression between *C. reinhardtii* cultured in N-replete and N-depleted medium was determined using the numbers of mapped reads overlapped with annotated *C. reinhardtii* genes as inputs to EdgeR (Robinson et al., 2010). In the Joint Genome Institute database, multiple sets of *C. reinhardtii* version 4 gene models are available. We used the "filtered" gene models, which contain the best gene model for each locus. Genes were regarded as differentially expressed if they have 2-fold or greater change between N-replete and N-deprived samples and 5% or less false discovery rate. Differential expressed genes were regarded as up-regulated if their expression levels in N-deprived samples were significantly higher than those in N-replete samples. Conversely, down-regulated genes were those with significantly lower levels of expression following N deprivation.

In addition to EdgeR, we used three other methods to evaluate differential expression: Fisher's exact test (Bloom et al., 2009), likelihood ratio test (Marioni et al., 2008), and a method based on intensity ratio and average intensity (MARS; Wang et al., 2010). All three methods were implemented in the DEGexp package (Wang et al., 2010). We found that among 4,004 differentially expressed genes called by EdgeR, 99.7% to 100% were regarded as differentially expressed by the other three methods. On the other hand, EdgeR calls overlap with 96.6%, 94.7%, and 95.8% of calls by Fisher's exact test, likelihood ratio test, and MARS, respectively. Our findings indicate that EdgeR is more conservative than the other methods, but the overall differential expression calls are highly similar among methods. We should note that methods other than EdgeR did not explicitly consider variance between replicates and, as a result, will likely have a higher false-positive differential expression call rate than that of EdgeR. Therefore, in all subsequent analyses, we used only EdgeR-based differential expression calls.

GO annotation for the *C. reinhardtii* version 4.0 genome was acquired from the Joint Genome Institute. Enrichment of differentially regulated genes in each GO category was determined using Fisher's exact test. To account for multiple testing, the *P* values from Fisher's exact tests were adjusted (Storey, 2003) and a false discovery rate of 5% was used as the threshold for enriched GO terms.

GC-MS Analysis

To quantify ^{13}C-labeling patterns such as mass-isotopomer distributions and fractional ^{13}C enrichment, samples were analyzed using GC-MS using an HP 6890 GC apparatus (Hewlett-Packard) equipped with DB-5MS column (5% phenyl-methyl-siloxan-diphenylpolysiloxan; 30 m × 0.251 mm × 0.25 μm; Agilent) and a quadrupole mass spectrometer (MS 5975; Agilent). Electron ionization was carried out at 70 eV. The obtained mass spectrometric data were corrected for the natural abundance of the elements to give fractional ^{13}C labeling.

Sampling, Extraction, and Analysis of Intracellular Amino Acid

Cells from TAP + N and TAP − N cultures were harvested after 24 h. This time point was chosen for these labeling experiments because at the required cell concentration (approximately 0.2 g cell dry weight L^{-1}) for metabolite extraction, acetate depletion occurs in cells grown in TAP + N at later time points due to the high initial inoculum.

The harvested cells (approximately 25 mg cell dry weight) were centrifuged at 3,000*g* for 1 min, and the supernatant was removed and quenched with 5 mL of cold 100% methanol (Winder et al., 2008). The metabolites were harvested by vortexing the cells. A second extraction was performed with 5 mL of chloroform:methanol (1:2). The extracts were then pooled. Water was slowly added to the pooled extracts for phase separation. The polar metabolites, which include the amino acids, were present in the aqueous phase. The aqueous phase was then dried under N_2 and converted to its *t*-butyldimethylsilyl derivative using *N*-methyl-*N*-(*t*-butyldimethylsilyl)trifluoroacetamide (Mawhinney et al., 1986). The GC and MS conditions for this analysis were as described previously (Deshpande et al., 2009).

Extraction and Analysis of Rib

Rib for analysis was obtained from the RNA as described (Boren et al., 2003). RNA was extracted from cells (0.1–0.2 g L^{-1}) at the same time point as the intracellular amino acids using the Tri reagent as described in the protocol (Molecular Research Center). The RNA was acid hydrolyzed to its monomers and dried under N. It was further analyzed using GC-MS by derivatizing it to its per-*O*-trimethylsilyl-*O*-ethyl oxime (MacLeod et al., 2001). The ions 481 to

486 (mass-to-charge ratio), corresponding to the whole carbon backbone of the Rib molecule (C_1–C_5), were monitored using single ion monitoring of the MS data.

Extraction and Analysis of Carbohydrate

The carbohydrates in the cells were acid hydrolyzed by 2 N HCl at 102°C, and the monomeric compounds were analyzed by GC-MS after the sample was dried under N_2. The sample was then converted to its di-*O*-isopropylidene acetate derivative for analysis by GC-MS (Hachey et al., 1999). The ions 287 to 293 (mass-to-charge ratio), corresponding to the whole carbon backbone of Glc (C_1–C_6), were monitored.

Sequence data from this article can be found in the National Center for Biotechnology Information Gene Expression Omnibus under accession numbers GSE24367, GSE2466, and GSE2465.

Supplemental Data

The following materials are available in the online version of this article.

Supplemental Table S1. Illumina analysis of transcripts related to gametogenesis.

Supplemental Table S2. Illumina analysis of transcripts related to N metabolism.

Supplemental Table S3. Illumina analysis of transcripts encoding chloroplast ribosomal proteins.

Supplemental Table S4. Illumina analysis of transcripts encoding cytosolic 80S ribosomal proteins.

Supplemental Table S5. Illumina analysis of transcripts encoding L22 ribosomal proteins.

Supplemental Table S6. Illumina analysis of transcripts encoding proteins of central metabolism.

Supplemental Table S7. Illumina analysis of transcripts related to photosynthesis.

Supplemental Table S8. Illumina analysis of transcripts related to lipid metabolism.

Supplemental Spreadsheet S1. Complete data set of all genes analyzed by 454 and Illumina.

ACKNOWLEDGMENTS

We thank Titus Brown, Gaurav Moghe, and Cheng Zou for help with analysis of Illumina data, James Bullard for help with comparing differential expression call methods, and the Joint Genome Institute for providing *C. reinhardtii* sequences and gene annotation.

Received August 31, 2010; accepted October 7, 2010; published October 8, 2010.

LITERATURE CITED

Athenstaedt K, Daum G (2005) Tgl4p and Tgl5p, two triacylglycerol lipases of the yeast Saccharomyces cerevisiae are localized to lipid particles. J Biol Chem **280:** 37301–37309

Baurain D, Dinant M, Coosemans N, Matagne RF (2003) Regulation of the alternative oxidase Aox1 gene in *Chlamydomonas reinhardtii*: role of the nitrogen source on the expression of a reporter gene under the control of the Aox1 promoter. Plant Physiol **131:** 1418–1430

Bloom JS, Khan Z, Kruglyak L, Singh M, Caudy AA (2009) Measuring differential gene expression by short read sequencing: quantitative comparison to 2-channel gene expression microarrays. BMC Genomics **10:** 221

Bonente G, Passarini F, Cazzaniga S, Mancone C, Buia MC, Tripodi M, Bassi R, Caffarri S (2008) The occurrence of the psbS gene product in Chlamydomonas reinhardtii and in other photosynthetic organisms and its correlation with energy quenching. Photochem Photobiol **84:** 1359–1370

Boren J, Lee WN, Bassilian S, Centelles JJ, Lim S, Ahmed S, Boros LG, Cascante M (2003) The stable isotope-based dynamic metabolic profile of butyrate-induced HT29 cell differentiation. J Biol Chem **278:** 28395–28402

Brady L, Brzozowski AM, Derewenda ZS, Dodson E, Dodson G, Tolley S, Turkenburg JP, Christiansen L, Huge-Jensen B, Norskov L, et al (1990) A serine protease triad forms the catalytic centre of a triacylglycerol lipase. Nature **343:** 767–770

Bullard JH, Purdom E, Hansen KD, Dudoit S (2010) Evaluation of statistical methods for normalization and differential expression in mRNA-Seq experiments. BMC Bioinformatics **11:** 94

Bulté L, Wollman FA (1992) Evidence for a selective destabilization of an integral membrane protein, the cytochrome b6/f complex, during gametogenesis in Chlamydomonas reinhardtii. Eur J Biochem **204:** 327–336

Camargo A, Llamas A, Schnell RA, Higuera JJ, González-Ballester D, Lefebvre PA, Fernández E, Galván A (2007) Nitrate signaling by the regulatory gene NIT2 in *Chlamydomonas*. Plant Cell **19:** 3491–3503

Carman GM, Han GS (2006) Roles of phosphatidate phosphatase enzymes in lipid metabolism. Trends Biochem Sci **31:** 694–699

Collier JL, Grossman AR (1992) Chlorosis induced by nutrient deprivation in Synechococcus sp. strain PCC 7942: not all bleaching is the same. J Bacteriol **174:** 4718–4726

Deshpande R, Yang TH, Heinzle E (2009) Towards a metabolic and isotopic steady state in CHO batch cultures for reliable isotope-based metabolic profiling. Biotechnol J **4:** 247–263

Eastmond PJ (2006) SUGAR-DEPENDENT1 encodes a patatin domain triacylglycerol lipase that initiates storage oil breakdown in germinating *Arabidopsis* seeds. Plant Cell **18:** 665–675

Emanuelsson O, Nielsen H, von Heijne G (1999) ChloroP, a neural network-based method for predicting chloroplast transit peptides and their cleavage sites. Protein Sci **8:** 978–984

Fernandez E, Llamas A, Galvan A (2009) Nitrogen assimilation and its regulation. *In* D Stern, EH Harris, eds, The Chlamydomonas Sourcebook: Organellar and Metabolic Processes, Ed 2, Vol 2. Elsevier, Dordrecht, The Netherlands, pp 69–113

Fisslthaler B, Meyer G, Bohnert HJ, Schmitt JM (1995) Age-dependent induction of pyruvate, orthophosphate dikinase in Mesembryanthemum crystallinum L. Planta **196:** 492–500

González-Ballester D, Camargo A, Fernández E (2004) Ammonium transporter genes in Chlamydomonas: the nitrate-specific regulatory gene Nit2 is involved in Amt1;1 expression. Plant Mol Biol **56:** 863–878

González-Ballester D, Casero D, Cokus S, Pellegrini M, Merchant SS, Grossman AR (2010) RNA-seq analysis of sulfur-deprived *Chlamydomonas* cells reveals aspects of acclimation critical for cell survival. Plant Cell **22:** 2058–2084

Hachey DL, Parsons WR, McKay S, Haymond MW (1999) Quantitation of monosaccharide isotopic enrichment in physiologic fluids by electron ionization or negative chemical ionization GC/MS using di-O-isopropylidene derivatives. Anal Chem **71:** 4734–4739

Hamel P, Olive J, Pierre Y, Wollman FA, de Vitry C (2000) A new subunit of cytochrome b6f complex undergoes reversible phosphorylation upon state transition. J Biol Chem **275:** 17072–17079

Harris EH (2009a) *Chlamydomonas* in the laboratory. *In* D Stern, EH Harris, eds, The Chlamydomonas Sourcebook: Introduction to Chlamydomonas and Its Laboratory Use, Ed 2, Vol 1. Elsevier, Dordrecht, The Netherlands, pp 241–302

Harris EH (2009b) The sexual cycle. *In* D Stern, EH Harris, eds, The Chlamydomonas Sourcebook: Introduction to Chlamydomonas and Its Laboratory Use, Ed 2, Vol 1. Elsevier, Dordrecht, The Netherlands, pp 119–157

Holm C, Osterlund T, Laurell H, Contreras JA (2000) Molecular mechanisms regulating hormone-sensitive lipase and lipolysis. Annu Rev Nutr **20:** 365–393

Hu Q, Sommerfeld M, Jarvis E, Ghirardi M, Posewitz M, Seibert M, Darzins A (2008) Microalgal triacylglycerols as feedstocks for biofuel production: perspectives and advances. Plant J **54:** 621–639

Jamers A, Van der Ven K, Moens L, Robbens J, Potters G, Guisez Y, Blust R, De Coen W (2006) Effect of copper exposure on gene expression

profiles in Chlamydomonas reinhardtii based on microarray analysis. Aquat Toxicol **80:** 249–260

Kanoh H, Sakane F, Imai S, Wada I (1993) Diacylglycerol kinase and phosphatidic acid phosphatase: enzymes metabolizing lipid second messengers. Cell Signal **5:** 495–503

Kurat CF, Natter K, Petschnigg J, Wolinski H, Scheuringer K, Scholz H, Zimmermann R, Leber R, Zechner R, Kohlwein SD (2006) Obese yeast: triglyceride lipolysis is functionally conserved from mammals to yeast. J Biol Chem **281:** 491–500

Kurvari V, Grishin NV, Snell WJ (1998) A gamete-specific, sex-limited homeodomain protein in Chlamydomonas. J Cell Biol **143:** 1971–1980

Langmead B, Trapnell C, Pop M, Salzberg SL (2009) Ultrafast and memory-efficient alignment of short DNA sequences to the human genome. Genome Biol **10:** R25

Ledford HK, Baroli I, Shin JW, Fischer BB, Eggen RI, Niyogi KK (2004) Comparative profiling of lipid-soluble antioxidants and transcripts reveals two phases of photo-oxidative stress in a xanthophyll-deficient mutant of Chlamydomonas reinhardtii. Mol Genet Genomics **272:** 470–479

Ledford HK, Chin BL, Niyogi KK (2007) Acclimation to singlet oxygen stress in Chlamydomonas reinhardtii. Eukaryot Cell **6:** 919–930

Li XP, Björkman O, Shih C, Grossman AR, Rosenquist M, Jansson S, Niyogi KK (2000) A pigment-binding protein essential for regulation of photosynthetic light harvesting. Nature **403:** 391–395

Li XP, Gilmore AM, Niyogi KK (2002) Molecular and global time-resolved analysis of a psbS gene dosage effect on pH- and xanthophyll cycle-dependent nonphotochemical quenching in photosystem II. J Biol Chem **277:** 33590–33597

MacLeod JK, Flanigan IL, Williams JF, Collins JG (2001) Mass spectrometric studies of the path of carbon in photosynthesis: positional isotopic analysis of (13)C-labelled C(4) to C(7) sugar phosphates. J Mass Spectrom **36:** 500–508

Majeran W, Wollman FA, Vallon O (2000) Evidence for a role of ClpP in the degradation of the chloroplast cytochrome b(6)f complex. Plant Cell **12:** 137–150

Mamedov TG, Moellering ER, Chollet R (2005) Identification and expression analysis of two inorganic C- and N-responsive genes encoding novel and distinct molecular forms of eukaryotic phosphoenolpyruvate carboxylase in the green microalga Chlamydomonas reinhardtii. Plant J **42:** 832–843

Marioni JC, Mason CE, Mane SM, Stephens M, Gilad Y (2008) RNA-seq: an assessment of technical reproducibility and comparison with gene expression arrays. Genome Res **18:** 1509–1517

Martin NC, Chiang KS, Goodenough UW (1976) Turnover of chloroplast and cytoplasmic ribosomes during gametogenesis in Chlamydomonas reinhardtii. Dev Biol **51:** 190–201

Martin NC, Goodenough UW (1975) Gametic differentiation in Chlamydomonas reinhardtii. I. Production of gametes and their fine structure. J Cell Biol **67:** 587–605

Mattingly SJ, Dipersio JR, Higgins ML, Shockman GD (1976) Unbalanced growth and macromolecular synthesis in Streptococcus mutans FA-1. Infect Immun **13:** 941–948

Mawhinney TP, Robinett RS, Atalay A, Madson MA (1986) Analysis of amino acids as their tert.-butyldimethylsilyl derivatives by gas-liquid chromatography and mass spectrometry. J Chromatogr A **358:** 231–242

Merchant SS, Prochnik SE, Vallon O, Harris EH, Karpowicz SJ, Witman GB, Terry A, Salamov A, Fritz-Laylin LK, Maréchal-Drouard L, et al (2007) The Chlamydomonas genome reveals the evolution of key animal and plant functions. Science **318:** 245–250

Moellering ER, Benning C (2010) RNA interference silencing of a major lipid droplet protein affects lipid droplet size in Chlamydomonas reinhardtii. Eukaryot Cell **9:** 97–106

Mus F, Dubini A, Seibert M, Posewitz MC, Grossman AR (2007) Anaerobic acclimation in Chlamydomonas reinhardtii: anoxic gene expression, hydrogenase induction, and metabolic pathways. J Biol Chem **282:** 25475–25486

Mussgnug JH, Wobbe L, Elles I, Claus C, Hamilton M, Fink A, Kahmann U, Kapazoglou A, Mullineaux CW, Hippler M, et al (2005) NAB1 is an RNA binding protein involved in the light-regulated differential expression of the light-harvesting antenna of *Chlamydomonas reinhardtii*. Plant Cell **17:** 3409–3421

Mustroph A, Lee SC, Oosumi T, Zanetti ME, Yang H, Ma K, Yaghoubi-Masihi A, Fukao T, Bailey-Serres J (2010) Cross-kingdom comparison of transcriptomic adjustments to low-oxygen stress highlights conserved and plant-specific responses. Plant Physiol **152:** 1484–1500

Nguyen AV, Thomas-Hall SR, Malnoë A, Timmins M, Mussgnug JH, Rupprecht J, Kruse O, Hankamer B, Schenk PM (2008) Transcriptome for photobiological hydrogen production induced by sulfur deprivation in the green alga Chlamydomonas reinhardtii. Eukaryot Cell **7:** 1965–1979

Oshlack A, Wakefield MJ (2009) Transcript length bias in RNA-seq data confounds systems biology. Biol Direct **4:** 14

Osterås M, Driscoll BT, Finan TM (1997) Increased pyruvate orthophosphate dikinase activity results in an alternative gluconeogenic pathway in Rhizobium (Sinorhizobium) meliloti. Microbiology **143:** 1639–1648

Peltier G, Schmidt GW (1991) Chlororespiration: an adaptation to nitrogen deficiency in Chlamydomonas reinhardtii. Proc Natl Acad Sci USA **88:** 4791–4795

Pérez-Rodríguez P, Riaño-Pachón DM, Corrêa LG, Rensing SA, Kersten B, Mueller-Roeber B (2010) PlnTFDB: updated content and new features of the plant transcription factor database. Nucleic Acids Res **38:** D822–D827

Plumley FG, Schmidt GW (1989) Nitrogen-dependent regulation of photosynthetic gene expression. Proc Natl Acad Sci USA **86:** 2678–2682

Pollard M, Ohlrogge J (1999) Testing models of fatty acid transfer and lipid synthesis in spinach leaf using in vivo oxygen-18 labeling. Plant Physiol **121:** 1217–1226

Riekhof WR, Benning C (2009) Glycerolipid biosynthesis. *In* DB Stern, EH Harris, eds, The Chlamydomonas Sourcebook: Organellar and Metabolic Processes, Ed 2, Vol 2. Elsevier, Dordrecht, The Netherlands, pp 41–68

Riekhof WR, Sears BB, Benning C (2005) Annotation of genes involved in glycerolipid biosynthesis in Chlamydomonas reinhardtii: discovery of the betaine lipid synthase BTA1Cr. Eukaryot Cell **4:** 242–252

Robinson MD, McCarthy DJ, Smyth GK (2010) EdgeR: a Bioconductor package for differential expression analysis of digital gene expression data. Bioinformatics **26:** 139–140

Schnell RA, Lefebvre PA (1993) Isolation of the Chlamydomonas regulatory gene NIT2 by transposon tagging. Genetics **134:** 737–747

Shockey JM, Fulda MS, Browse JA (2002) Arabidopsis contains nine long-chain acyl-coenzyme A synthetase genes that participate in fatty acid and glycerolipid metabolism. Plant Physiol **129:** 1710–1722

Shrager J, Hauser C, Chang CW, Harris EH, Davies J, McDermott J, Tamse R, Zhang Z, Grossman AR (2003) Chlamydomonas reinhardtii genome project: a guide to the generation and use of the cDNA information. Plant Physiol **131:** 401–408

Siersma PW, Chiang KS (1971) Conservation and degradation of cytoplasmic and chloroplast ribosomes in Chlamydomonas reinhardtii. J Mol Biol **58:** 167–172

Simon DF, Descombes P, Zerges W, Wilkinson KJ (2008) Global expression profiling of Chlamydomonas reinhardtii exposed to trace levels of free cadmium. Environ Toxicol Chem **27:** 1668–1675

Storey JD (2003) The positive false discovery rate: a Bayesian interpretation and the *q*-value. Ann Stat **31:** 2013–2035

Taylor L, Nunes-Nesi A, Parsley K, Leiss A, Leach G, Coates S, Wingler A, Fernie AR, Hibberd JM (2010) Cytosolic pyruvate,orthophosphate dikinase functions in nitrogen remobilization during leaf senescence and limits individual seed growth and nitrogen content. Plant J **62:** 641–652

Trapnell C, Pachter L, Salzberg SL (2009) TopHat: discovering splice junctions with RNA-Seq. Bioinformatics **25:** 1105–1111

Trapnell C, Williams BA, Pertea G, Mortazavi A, Kwan G, van Baren MJ, Salzberg SL, Wold BJ, Pachter L (2010) Transcript assembly and quantification by RNA-Seq reveals unannotated transcripts and isoform switching during cell differentiation. Nat Biotechnol **28:** 511–515

Wang L, Feng Z, Wang X, Wang X, Zhang X (2010) DEGseq: an R package for identifying differentially expressed genes from RNA-seq data. Bioinformatics **26:** 136–138

Wang ZT, Ullrich N, Joo S, Waffenschmidt S, Goodenough U (2009) Algal lipid bodies: stress induction, purification and biochemical characterizatioon in wild-type and starch less *Chlamydomonas reinhardtii*. Eukaryot Cell **8:** 1856–1868

Weber AP, Weber KL, Carr K, Wilkerson C, Ohlrogge JB (2007) Sampling the Arabidopsis transcriptome with massively parallel pyrosequencing. Plant Physiol **144:** 32–42

Wijffels RH, Barbosa MJ (2010) An outlook on microalgal biofuels. Science **329:** 796–799

Winder CL, Dunn WB, Schuler S, Broadhurst D, Jarvis R, Stephens GM, Goodacre R (2008) Global metabolic profiling of Escherichia coli cultures: an evaluation of methods for quenching and extraction of intracellular metabolites. Anal Chem **80:** 2939–2948

Winkler FK, D'Arcy A, Hunziker W (1990) Structure of human pancreatic lipase. Nature **343:** 771–774

Wu TD, Watanabe CK (2005) GMAP: a genomic mapping and alignment program for mRNA and EST sequences. Bioinformatics **21:** 1859–1875

Yamano T, Miura K, Fukuzawa H (2008) Expression analysis of genes associated with the induction of the carbon-concentrating mechanism in *Chlamydomonas reinhardtii*. Plant Physiol **147:** 340–354

Zimmermann R, Strauss JG, Haemmerle G, Schoiswohl G, Birner-Gruenberger R, Riederer M, Lass A, Neuberger G, Eisenhaber F, Hermetter A, et al (2004) Fat mobilization in adipose tissue is promoted by adipose triglyceride lipase. Science **306:** 1383–1386